

# A Prototype Preceding Vehicle Identification System Development and Field Evaluation

Zeyu Mu<sup>1</sup><sup>a</sup>, Guancheng Tu<sup>2</sup>, Austin Shi<sup>2</sup>, Kun Yang<sup>3</sup>, Yixin Sun<sup>4</sup>, Cong Shen<sup>3</sup> and B. Brian Park<sup>5</sup><sup>b</sup>

<sup>1</sup>Department of Systems & Information Engineering, University of Virginia, Charlottesville, VA, U.S.A.

<sup>2</sup>Department of Computer Science, University of Virginia, Charlottesville, VA, U.S.A.

<sup>3</sup>Department of Electrical & Computer Engineering, University of Virginia, Charlottesville, VA, U.S.A.

<sup>4</sup>Departments of Computer Science and Electrical & Computer Engineering, University of Virginia, Charlottesville, VA, U.S.A.

<sup>5</sup>Departments of Civil & Environmental Engineering and Systems & Information Engineering, University of Virginia, Charlottesville, VA, U.S.A.

**Keywords:** Connected Vehicles, Vehicle-to-Vehicle Communication, Preceding Vehicle Identification System, Field Test.


**Abstract:** Preceding vehicle identification is crucial for establishing cooperative platooning. This paper presents the development of a prototype preceding vehicle identification system (PVIS) and its field evaluation for the assessment of commercial viability. We designed and assembled a prototype consisting of a processing unit (Jetson Nano board), a communication device (Wi-Fi dongle), a GPS unit, and a distance measurement sensor (Terabee sensor). The Jetson Nano integrates the SparkFun GPS-RTK-SMA unit, the Terabee time-of-flight sensor, and the Wi-Fi dongle. The PVIS prototype in the ego vehicle measures the distance to its preceding vehicle and receives the GPS data from potential preceding vehicles with the PVIS prototypes. With these, the PVIS in the ego vehicle determines the connectivity of the preceding vehicle. The field evaluation results showed that the prototype PVIS works as designed, and each successful identification takes about 5.3 seconds. However, it was found that the Terabee (time of flight) sensor, at times, did not properly measure distances, likely due to an angle issue caused by the roadway surface and vibration of the vehicle. We discussed how to overcome the challenges identified and enhance the prototype for successful commercialization.


## 1 INTRODUCTION

The National Highway Traffic Safety Administration (NHTSA) reported that motor vehicle crashes impose a substantial economic burden of \$340 billion annually on American society (Blincoe et al., 2023). The analysis encompasses the costs associated with one year of crashes, resulting in the tragic loss of an estimated 36,500 lives, injuries to 4.5 million individuals, and damage to 23 million vehicles. Connected and automated vehicle (CAV) is a transformative technology that has great potential for reducing traffic crashes, enhancing the quality of life, and improving the efficiency of transportation systems (Mu et al., 2022; Matin and Dia, 2023). A pivotal technique employed by CAVs is cooperative platooning, wherein these vehicles communicate and cooperate

with the connected preceding vehicle to form a cohesive string-like arrangement. Such a cooperative platoon relies on Vehicle-to-Vehicle (V2V) communication, which has the potential to significantly mitigate or prevent 80% of collisions involving unimpaired drivers (Harding et al., 2014) and improve the traffic capacity and mobility (Van Arem et al., 2006; Chang et al., 2020).

V2V communication employs a Cellular Vehicle-to-Everything (C-V2X) technology, enabling messages to be shared among connected vehicles (CVs). The transmitted messages include the essential Basic Safety Messages (BSM) such as the current Global Positioning System (GPS) coordinates, speed, acceleration, and heading. Additionally, these messages convey vehicle control information, incorporating details such as transmission state, brake status, and steering wheel angle. Despite its essential role in facilitating communication, the BSM does not incorporate information such as preceding vehicle ID or lane

<sup>a</sup> <https://orcid.org/0000-0003-0957-0061>

<sup>b</sup> <https://orcid.org/0000-0003-4597-6368>

ID. Achieving this precise identification relies on the utilization of an accurate GPS position shared by the preceding vehicle through V2V communication. This potentially enables the CAV to effectively pinpoint the location of the connected preceding vehicle. However, the usage of commercial GPS devices is constrained by the potential occurrence of significant position errors, ranging from 1 to 4 meters (El Abbous and Samanta, 2017).

The critical nature of accurate identification becomes apparent, as an erroneous identification because of the large GPS error could lead the CAV to establish cooperation with a nearby connected vehicle rather than the intended preceding vehicle. Such misidentification poses a significant risk, potentially resulting in unsafe and precarious situations within the vehicular environment. Ensuring the precision of the identification process is paramount, as it directly influences the reliability of cooperative interactions between CAVs and their immediate predecessors, ultimately safeguarding the integrity and safety of the connected driving experience.

Existing research about preceding vehicle identification systems mainly focuses on simulation in fully connected environments (Kobayashi et al., 2019; Sakaguchi et al., 2023). However, in the imminent future, the coexistence of human-driven vehicles and CVs introduces a noteworthy challenge in accurately identifying connected preceding vehicles. To overcome the limitation mentioned above, a preceding vehicle identification system (PVIS) (Chen and Park, 2022) is developed for CAVs to identify the connected preceding vehicle utilizing GPS-measured distance and sensor-measured distance on a road with multiple lanes under mixed traffic. The fundamental concept underlying PVIS is the iterative matching of GPS-measured distances and sensor-measured distances (smaller than a predefined threshold), performed multiple times to achieve a low misidentification rate. The threshold and time are optimized intricately tied to the distribution of GPS and sensor errors, ensuring that the matching process occurs at opportune moments, thereby balancing the accuracy of the system and the time consumption (Chen and Park, 2022). The system showed its advances in identifying the connected preceding vehicle through simulation. However, while simulation provides valuable insights, it inherently simplifies the complexity of real-world traffic scenarios such as GPS and sensor errors and communication efficiency, highlighting the need for more intricate simulations that better mirror the intricate dynamics of multi-lane traffic conditions. Transitioning from simulation to practical implementation ensures that the system's efficacy and reliability

are thoroughly assessed in authentic and dynamic environments.

Previous research (Chen and Park, 2022) proved the efficiency of the PVIS in the simulation, however, to the best of our knowledge, no prior research has been conducted on preceding vehicle identification in real-world field conditions. This paper introduces a novel contribution by proposing the design of a prototype and undertaking an evaluation of a preceding vehicle identification system in a practical, field-based setting. The prototype consists of a processing unit (Jetson Nano board), a communication device (Wi-Fi dongle), a GPS unit, and a distance measurement sensor (Terabee time-of-flight (ToF) sensor). Two connected human-driven vehicles are assembled with the prototype system for testing as shown in Fig. 1. Transitioning from controlled environments to the unpredictable dynamics of the real world, the system's performance is scrutinized from different perspectives such as accuracy, algorithm efficiency, and communication efficiency, aiming to assess its robustness and reliability. This endeavor is not only a technical evaluation but also a pivotal exploration of the system's practicality and effectiveness in addressing the challenges posed by commercial devices. This paper aims to shed light on the practical implications and performance of the preceding vehicle identification system in real-world conditions.

The paper outline is shown as follows: Section 2 PROTOTYPE DESIGN presents the prototype including the hardware platform (Jetson Nano) with the Wi-Fi dongle, the GPS devices, and the distance measurement sensor (Terabee sensor). Section 3 EXPERIMENTS AND RESULTS illustrated the experiment settings and experimental results. Section 4 CONCLUSIONS AND FUTURE WORK presented the conclusions and future work.

## 2 PROTOTYPE DESIGN

The PVIS system stands as a pivotal technology for fostering cooperation between the ego CAV and its connected preceding vehicle. This system hinges on the sensor-derived distance between the ego CAV and its preceding counterpart, augmented by GPS position data obtained through V2V communication. With the primary objective centered on evaluating the commercial viability of the prototype, meticulous considerations are made in selecting the processing unit, sensor, and GPS device. The hardware platform is tasked with algorithm computation, data processing, sharing, and interfacing with the sensor and GPS devices. The chosen components prioritize reliability, security, and

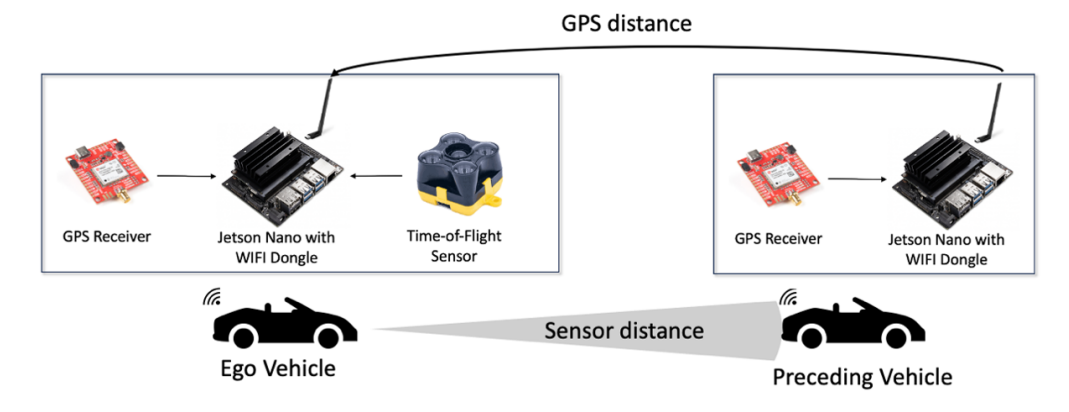


Figure 1: Prototype Preceding Vehicle Identification System.

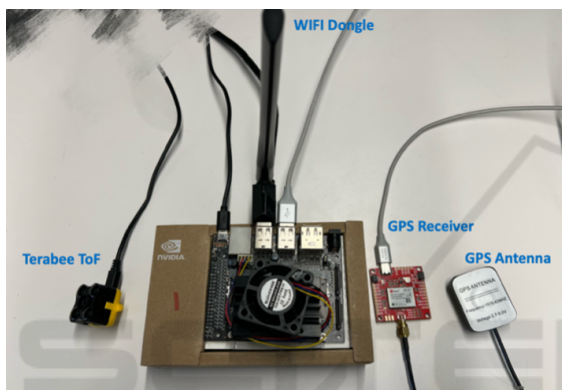


Figure 2: Hardware Platform with Wi-Fi dongle, GPS receiver, and Terabee ToF.

real-time functionality, ensuring the robust and secure execution of the PVIS system for practical applications.

## 2.1 Hardware Platform

Computers have evolved into highly versatile hardware, continuously advancing since their inception. In the applications of robotics or autonomous driving, there is a preference for compact, portable, cost-effective, and high-performance computing solutions, deviating from the high-cost and physically cumbersome traditional computers. Therefore, single-board computers (SBC) such as NVIDIA Jetson Nano and Raspberry Pi have gained prominence. These computers are constructed on a solitary circuit board and integrate microprocessors, memory, input/output interfaces, and other essential functionalities (Isikdag, 2015).

In a comparative analysis between Raspberry Pi and NVIDIA Jetson Nano, it is observed that Raspberry Pi stands out for its low power consumption and energy-efficient performance. However, the study

concludes that NVIDIA Jetson platforms, particularly exemplified by the Jetson Nano, exhibit superior overall performance. This performance superiority is attributed to the presence of higher-speed Graphics Processing Units (GPUs) in the Jetson platform, emphasizing the pivotal role of advanced GPU capabilities in achieving heightened computational power compared to (Ullah and Kim, 2020).

In a comparative analysis with the Jetson Orin NX, it is determined that the Jetson Nano is a more cost-effective and suitable solution for the current functional requirements of the research. Therefore, the selected hardware platform is the NVIDIA Jetson Nano, featuring an Intel Core i7-4790 CPU at 3.60 GHz, a GeForce RTX 2080 GPU with 8 GB VRAM, 16 GB of RAM, and operating on Ubuntu 18.04. Supplementary components, including a Wi-Fi dongle, vehicle sensors, and a GPS receiver, were integrated into this hardware setup, as illustrated in Fig. 2. The Jetson Nano played a central role in facilitating communication between CVs, executing algorithm calculations, and processing data. Specifically, the Jetson Nano on the ego vehicle functions as a Wi-Fi access point in ad-hoc mode, creating a network that other vehicles can connect to. The preceding vehicle, equipped with a Wi-Fi dongle, establishes a connection to the ad-hoc Wi-Fi network generated by the Jetson Nano on the ego vehicle. Wi-Fi and C-V2X technology are both designed for wireless short-range communication and operate based on established communication standards. However, C-V2X typically demands a significant infrastructure deployment, while Wi-Fi offers a more commercially viable solution for field tests. Wi-Fi has proven to be a successful communication medium between vehicles, even at very high speeds, such as 120 mph relative speed (Tufail et al., 2008).

## 2.2 GPS Receiver

The GPS stands as the singular, fully operational Global Navigation Satellite System (GNSS), relying on a constellation of 24 to 32 Medium Earth Orbit satellites. These satellites transmit precise microwave signals, empowering GPS receivers to ascertain their location, speed, direction, and time. For distance calculation, a GPS receiver necessitates signals from a minimum of three satellites, utilizing a triangulation technique to compute its two-dimensional position (latitude and longitude). Leveraging the self-reported GPS location of the ego Connected Vehicle (CV) and the shared GPS locations of other CVs, the ego CV can compute the relative distance between two vehicles based on these GPS reports. This GPS-derived measurement serves as a pivotal reference point, allowing for comparison with sensor-measured distances and facilitating the identification of the preceding vehicle within the vehicle platoon.

After a comprehensive examination of various GPS modules, including Beffkip, BerryGPS, Wave-share, and SparkFun, the SparkFun GPS-RTK-SMA was chosen for implementation. This decision was influenced by several pivotal factors. Firstly, the SparkFun GPS features an impressive maximum update rate of 20 HZ, providing more frequent and real-time location data compared to the standard 1 HZ update rate offered by other GPS units. Furthermore, the SparkFun GPS unit's type-C port facilitates a straightforward and direct connection to the Jetson Nano, eliminating the necessity for additional wires and GPIO connections, a feature not always present in modules primarily designed for Raspberry Pi, such as BerryGPS.

## 2.3 Vehicle Sensor

Vehicle sensors play a pivotal role in furnishing both a perceptive and locational understanding of the environment, facilitating real-time decision-making for the vehicle (Campbell et al., 2018) deployment of various types of vehicle sensors caters to diverse objectives in real traffic scenarios. Each type of sensor contributes distinct functionalities, collectively enhancing the vehicle's capability to sense, interpret, and respond to its dynamic surroundings. LiDAR sensors, functioning on the principle of time of flight (TOF), utilize laser beams to measure distances and generate detailed three-dimensional maps of the environment. Radar sensors utilize radio waves to detect objects and determine their range, speed, and direction, effective in tracking the movement of vehicles. Cameras capture visual information and enable the identification

of traffic signs, lane markings, and the classification of objects such as vehicles, pedestrians, and cyclists.

In this research, the TeraRanger Evo 60m sensor is selected as the vehicle sensor for system development. The decision is driven by the sensor's cost-efficiency, ease of integration, reliable performance, and ability to fulfill the proper measurement requirements of the research. Key features of the TeraRanger Evo 60m sensor include its ability to measure distances up to 60 meters, provide a high sampling rate of up to 240 readings per second, and encompass a field of view spanning 2 degrees. Notably, the sensor demonstrates impressive accuracy, with an error of less than 0.1 m. Hence, the accuracy and frequency of the ToF sensor are deemed acceptable for this study, with performance characteristics surpassing those of GPS. The straightforward integration involves a simple plug-and-play mechanism, connecting to the SBC via USB. This direct connectivity eliminates the need for adapters or intricate wiring, streamlining the implementation process.

## 3 EXPERIMENTS AND RESULTS

### 3.1 Methodology

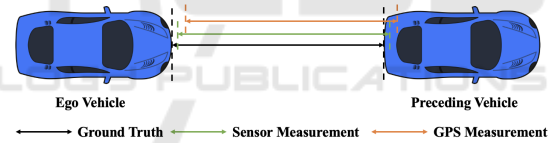


Figure 3: Ground truth, sensor and GPS measurements between the ego vehicle and the preceding vehicle.

For the PVIS (Chen and Park, 2022) to achieve both safety and efficiency, three main factors are taken into consideration: the probability of misidentifying another connected vehicle as the preceding vehicle, the probability of misidentifying the preceding vehicle as unconnected, and the time consumption. The PVIS iteratively matches the GPS-measured gap between the preceding vehicle and the ego vehicle with the sensor-measured gap in Fig. 3. The process of iteration for matching to identify connected and unconnected preceding vehicles ( $n$  and  $k$ , respectively) is detailed in Fig. 4. The threshold of matching, difference between the GPS measured-distance and sensor-measured distance ( $e$ ), is defined in Eq. 1.

$$e = \left( \frac{\Delta d_g - \Delta d_s}{\delta} \right)^2 = \left( \frac{e_g - e_s}{\delta} \right)^2 < inv\chi^2(1, \alpha) \quad (1)$$



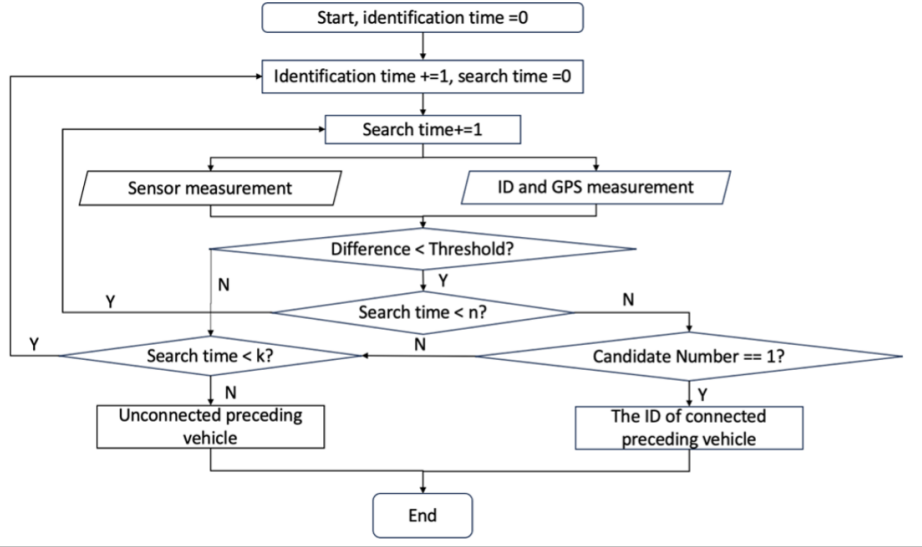


Figure 4: Flowchart of Identification Procedure.

Where  $\Delta d$  represents the distance difference between the ego vehicle and the preceding vehicle. The subscripts  $g$  and  $s$  indicate variables related to GPS and sensor measurements, respectively.  $e$  denotes the difference between the measurements and the ground truth. The standard deviations for the difference between GPS and sensor measurements is represented by  $\delta$ .  $inv\chi^2$  signifies the inverse-chi-square distribution with 1 degree of freedom, and  $\alpha$  determines the threshold of matching based on the Chi-square distribution. It is noted that as the TOF sensor provides the relative distance between two vehicles, the combination of GPS and TOF sensor measurements can be modeled by the inverse-chi-square distribution with 1 degree of freedom.

The most critical factor, probability of misidentifying another connected vehicle as the connected preceding vehicle,  $Er$ , is defined in Eqs. 2 and 3. This probability represents scenarios where any nearest connected vehicles in adjacent lanes fall within the matching threshold for  $n$  consecutive iterations. Such misidentification can lead to potential safety issues by initiating cooperation with the incorrect connected vehicle.

$$Er \approx 2k \left( \int_A f(e) de \right)^n \quad (2)$$

$$A = \{e | e - w \leq e \leq e + w\} \quad (3)$$

where  $f(e)$  is the probability density function of normal distribution for measurement errors;  $w$  is the minimum distance between preceding vehicle and the nearest preceding vehicle. The second critical factor, the probability of misidentifying the preceding vehicle as unconnected,  $Ur$ , is defined as Eq. 4, representing the corrected connected preceding vehicle is not

within the threshold for  $n$  consecutive times repeated in  $k$  consecutive times.

$$Ur = (1 - (1 - \alpha)^n)^k \quad (4)$$

The maximum time for the identification can be determined to be  $0.1nk$  seconds, considering that connected vehicles share their GPS data every 0.1 seconds. To balance the accuracy and time consumption of identification, the parameters related to threshold and times of iterations ( $\alpha, n$  and  $k$ ) of PVIS are optimized in relation to the optimization problem, formulated in Eq. 5.

$$\begin{aligned} \min_{\alpha, n, k} \quad & w_1 Ur + w_2 T \\ \text{s.t.} \quad & Ur \leq Ur_{max} \\ & Er \leq Er_{max} \\ & T = 0.1nk \leq T_{max} \\ & 0 \leq \alpha \leq 1 \\ & n, k \in N^+ \end{aligned} \quad (5)$$

where  $w_1$  and  $w_2$  are weights of the probability of identifying the preceding vehicle as an unconnected vehicle and time consumption, respectively.  $Er_{max}$ ,  $Ur_{max}$  and  $T_{max}$  are maximum value of  $Er$ ,  $Ur$  and  $T$ , respectively.

### 3.2 Proof-of-Concept Field Test

For the field test, it's crucial to initially establish the parameters of the Preceding Vehicle Identification System (PVIS), as depicted in Fig. 4. The error assumptions for the GPS devices and Time-of-Flight (ToF) sensor are based on their documentation, where GPS and ToF sensor errors are presumed



Figure 5: Two connected human-driven vehicles in the parking lot.

to follow a normal distribution with standard deviations of 2.5 and 0.1, respectively. Furthermore, the parameters  $Er_{max}$ ,  $Ur_{max}$ ,  $T_{max}$  and are configured as  $10^{-8}$ , 0.05, and 60 seconds, respectively;  $w_1$ ,  $w_2$ , and  $w$  are set to be 500, 1 and 2.5 meters respectively. Referring to Eq. 5, the times of iterations ( $n$  and  $k$ ) and  $\alpha$  related threshold are optimized to 60, 10, and  $inv\chi^2(1, 0.017) = 5.7$ .

In the field tests, two human-driven vehicles served as CVs. The Jetson Nano for both vehicles was positioned below the front windows to ensure a stable connection between the two vehicles. The Jetson Nano on each vehicle was interfaced with a Wi-Fi dongle and a GPS receiver. To precisely measure the gap between the front of the ego vehicle and the rear end of the preceding vehicle, the GPS antenna for the ego vehicle was placed at the front, while the GPS antenna for the preceding vehicle was positioned at the rear end, as illustrated in Fig. 5. It is noteworthy that the GPS antenna on each vehicle was mounted on the bonnet to ensure an unobstructed view for receiving GPS information. The ToF sensor is located at the front of the ego vehicle for enhanced distance measurement accuracy. For safety considerations, two connected human-driven vehicles were operated in a parking lot at a deliberately low speed (less than 10 mph). It's worth noting that higher speeds between vehicles could result in longer distances between them. However, the accuracy of GPS is not highly influenced by the distance between vehicles in open-sky conditions. The straight road within the parking lot extended approximately 600 meters.

### 3.3 Experimental Results

To assess the reliability and commercial viability of the prototype PVIS, various metrics are evaluated, encompassing the accuracy of GPS and Time-of-Flight (ToF) sensor measurements, system accuracy and efficiency, communication delay, and security considerations. Specifically, distance measurements from both the GPS and ToF sensors are collected to gauge the error of these devices. The identification accuracy and time consumption metrics are gathered to assess overall system accuracy and efficiency. The timeline between the moment the preceding vehicle acquires GPS information and the subsequent moment the ego vehicle receives this GPS information is measured to calculate communication delay. This methodology allows for a comprehensive assessment of the identification system's resilience in the face of varying connection densities and potential malicious attacks.

Multiple identification tests were systematically conducted, resulting in the collection of 2,732 pairs of GPS and sensor data. Throughout the tests, the gap between the two vehicles remained below 10 meters, and their speed was constrained to be less than 5 m/s. During the tests, an observed sensitivity of the ToF sensor to variations in road surface and angle was noted. Specifically, the sensor returned invalid values when the vehicle traversed an irregular roadway surface, leading to a small percentage of data being deemed invalid. In the remaining valid data (i.e., 2,618 pairs) derived from 43 tests, the ego vehicle demonstrates a 100% success rate in identifying the preceding vehicle across 43 tests. The mean

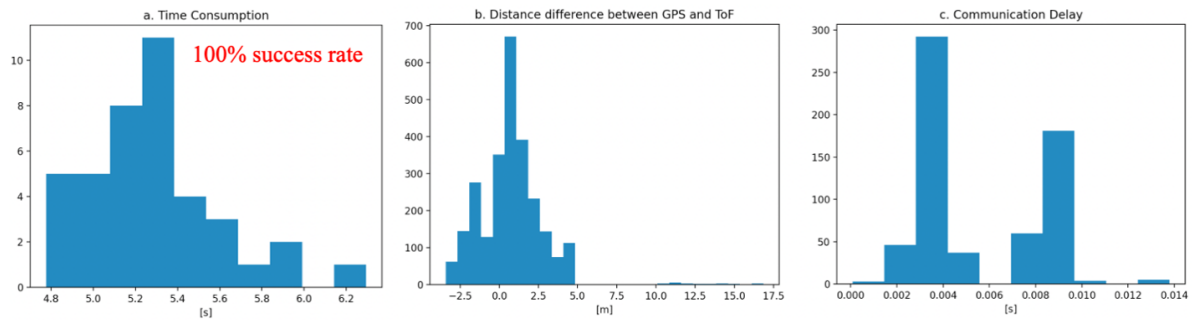


Figure 6: Histogram of time consumption, distance difference between the GPS and ToF sensors, and communication delay in 43 tests.

and standard derivation of the consumption time is 5.3 seconds and 0.32, respectively, as shown in Fig. 6.a. A histogram representing the measured distance differences between the GPS and ToF sensor is depicted in Fig. 6.b. The mean and standard deviation of the distance differences between the GPS and ToF sensor are calculated to be 0.8 and 2.1, respectively. Discrepancies between the collected data and the error distribution outlined in the documentation may be attributed to the possibility that the data does not comprehensively cover all real-world scenarios. Environmental factors can influence the performance of GPS and radar devices, contributing to variations in the collected data.

The communication delay is shown in Fig. 6.c. The communication delay refers to the time difference between the time when the ego vehicle receives GPS location and the time when the preceding gains its self-reported GPS. Based on the field test, the mean and the standard deviation of the communication delay are 0.0055 and 0.0026, respectively, which means the communication delay is negligible compared to the time of each identification step (around 0.1 seconds).

### 3.4 Reassessment with Observed Data

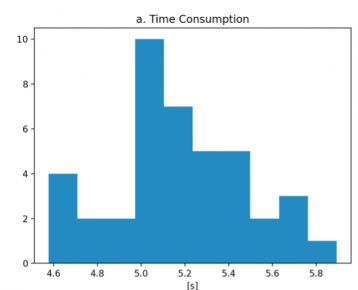


Figure 7: Histogram of time consumption with reoptimized PVIS settings.

As illustrated in Fig. 6.b, the observed error distribu-

tion of GPS and the sensor deviates from the initial assumption. Given the impact of this error distribution on the efficiency of the PVIS, a reassessment based on observed data becomes crucial for its effective implementation. Therefore, a re-optimization of parameters was undertaken based on the observed error distribution. The actual error distribution has a mean of 0.8 and a standard deviation of 2.1. The reoptimized parameters, namely  $n = 59$ ,  $k = 9$  and threshold at 5.4, were determined based on the optimization problem in the paper (Chen and Park, 2022). Subsequently, the data collected from the field was reanalyzed using these new parameters. The data from 43 tests resulted in a 100% successful rate. The mean and standard deviation of the time consumption for identification were found to be 5.2 seconds and 0.31, respectively, as illustrated in Fig. 7. These adjustments reflect a small improvement in time consumption under the updated error distribution.

## 4 CONCLUSIONS AND FUTURE WORK

This paper undertook the development and evaluation of a prototype preceding vehicle identification system in a real-world setting. Human-driven vehicles, equipped with Jetson Nano and integrated with a Wi-Fi dongle, GPS receiver, and ToF sensor, served as connected vehicles. The performance of the prototypes underwent assessment, focusing on the accuracy of GPS and ToF sensor measurements, system accuracy and efficiency, and communication delay considerations. The results demonstrate that the system requires approximately 5.3 seconds to successfully identify the connected preceding vehicle, utilizing a commercial GPS receiver and ToF sensor. The system achieved 100% accuracy in 43 identification tests, with negligible communication delay observed. The PVIS was reassessed based on the observed er-

ror distribution, which proved to be smaller than the initial assumption. This resulted in shorter time consumption for identification, specifically 5.2 seconds, showcasing improved efficiency under the updated parameter settings.

However, some challenges need to be investigated in the future. Firstly, the sensitivity and narrow 2° Field of View of the Terabee ToF sensor posed limitations during testing, as it returned invalid data when the vehicle traversed uneven terrain and experienced vibrations. Addressing these issues is crucial to ensure the reliable and robust performance of the Terabee ToF sensor in varying driving conditions. Potential solutions may involve exploring alternative sensor technologies that are less susceptible to these environmental factors or improving the sensor's installation for stability. Additionally, it's important to note that the field test in this study involved two vehicles, serving as a proof of concept. To further ensure the comprehensiveness and applicability of the algorithm, future testing efforts should strive for environments that include a diverse mix of multiple vehicles.

## ACKNOWLEDGEMENTS

This research is supported by the National Science Foundation (Grant CMMI-2009342), the Commonwealth Cyber Initiative, the SMARTER University Transportation Center, and the Virginia Transportation Research Council.

## REFERENCES

- Blincoe, L., Miller, T., Wang, J.-S., Swedler, D., Coughlin, T., Lawrence, B., Guo, F., Klauer, S., and Dingus, T. (2023). *The Economic and Societal Impact of Motor Vehicle Crashes, 2019 (Revised)*.
- Campbell, S., O'Mahony, N., Krpalcova, L., Riordan, D., Walsh, J., Murphy, A., and Ryan, C. (2018). Sensor technology in autonomous vehicles : A review. In *2018 29th Irish Signals and Systems Conference (ISSC)*, pages 1–4.
- Chang, X., Li, H., Rong, J., Zhao, X., and Li, A. (2020). Analysis on traffic stability and capacity for mixed traffic flow with platoons of intelligent connected vehicles. *Physica A: Statistical Mechanics and its Applications*, 557:124829.
- Chen, Z. and Park, B. B. (2022). Connected preceding vehicle identification for enabling cooperative automated driving in mixed traffic. 148(5):04022013. Publisher: American Society of Civil Engineers.
- El Abbous, A. and Samanta, N. (2017). A modeling of gps error distributions. In *2017 European Navigation Conference (ENC)*, pages 119–127.
- Harding, J., Powell, G. H., Yoon, R., Fikentscher, J., Doyle, C., Sade, D., Lukuc, M., Simons, J., and Wang, J. (2014). Vehicle-to-vehicle communications: Readiness of v2v technology for application.
- Isikdag, U. (2015). Internet of things: Single-board computers. In Isikdag, U., editor, *Enhanced Building Information Models: Using IoT Services and Integration Patterns*, SpringerBriefs in Computer Science, pages 43–53. Springer International Publishing.
- Kobayashi, H., Han, K., and Kim, B. (2019). Vehicle-to-vehicle message sender identification for co-operative driver assistance systems. In *2019 IEEE 89th Vehicular Technology Conference (VTC2019-Spring)*, pages 1–5. ISSN: 2577-2465.
- Matin, A. and Dia, H. (2023). Impacts of connected and automated vehicles on road safety and efficiency: A systematic literature review. 24(3):2705–2736. Conference Name: IEEE Transactions on Intelligent Transportation Systems.
- Mu, Z., Chen, Z., Ryu, S., Avedisov, S. S., Guo, R., and Park, B. B. (2022). Cooperative platooning with mixed traffic on urban arterial roads. In *2022 IEEE Intelligent Vehicles Symposium (IV)*, pages 1578–1583.
- Sakaguchi, Y., Bakibillah, A. S. M., Kamal, M. A. S., and Yamada, K. (2023). A cyber-physical framework for optimal coordination of connected and automated vehicles on multi-lane freeways. 23(2):611. Number: 2 Publisher: Multidisciplinary Digital Publishing Institute.
- Tufail, A., Fraser, M., Hammad, A., Hyung, K. K., and Yoo, S.-W. (2008). An empirical study to analyze the feasibility of WIFI for VANETs. In *2008 12th International Conference on Computer Supported Cooperative Work in Design*, pages 553–558.
- Ullah, S. and Kim, D.-H. (2020). Benchmarking jetson platform for 3d point-cloud and hyper-spectral image classification. In *2020 IEEE International Conference on Big Data and Smart Computing (BigComp)*, pages 477–482. ISSN: 2375-9356.
- Van Arem, B., van Driel, C. J. G., and Visser, R. (2006). The impact of cooperative adaptive cruise control on traffic-flow characteristics. *IEEE Transactions on Intelligent Transportation Systems*, 7(4):429–436.